© 2015. Published by The Company of Biologists Ltd | Journal of Cell Science (2015) 128, 2057-2069 doi:10.1242/jcs.160341

RESEARCH ARTICLE

Sphingolipids inhibit vimentin-dependent cell migration

Claire L. Hyder[1,2,*], Kati Kemppainen[2,*], Kimmo O. Isoniemi[1,2], Susumu Y. Imanishi[1,3], Hidemasa Goto[4,5], Masaki Inagaki[4,5], Elnaz Fazeli[2], John E. Eriksson[1,2,‡] and Kid Törnquist[2,6,‡]

ABSTRACT

The sphingolipids, sphingosine 1-phosphate (S1P) and sphingosylphosphorylcholine (SPC), can induce or inhibit cellular migration. The intermediate filament protein vimentin is an inducer of migration and a marker for epithelial–mesenchymal transition. Given that keratin intermediate filaments are regulated by SPC, with consequences for cell motility, we wanted to determine whether vimentin is also regulated by sphingolipid signalling and whether it is a determinant for sphingolipid-mediated functions. In cancer cells where S1P and SPC inhibited migration, we observed that S1P and SPC induced phosphorylation of vimentin on S71, leading to a corresponding reorganization of vimentin filaments. These effects were sphingolipid-signalling-dependent, because inhibition of either the $S1P_2$ receptor (also known as S1PR2) or its downstream effector Rho-associated kinase (ROCK, for which there are two isoforms ROCK1 and ROCK2) nullified the sphingolipid-induced effects on vimentin organization and S71 phosphorylation. Furthermore, the anti-migratory effect of S1P and SPC could be prevented by expressing S71-phosphorylation-deficient vimentin. In addition, we demonstrated, by using wild-type and vimentin-knockout mouse embryonic fibroblasts, that the sphingolipid-mediated inhibition of migration is dependent on vimentin. These results imply that this newly discovered sphingolipid–vimentin signalling axis exerts brake-and-throttle functions in the regulation of cell migration.

KEY WORDS: S1P, SPC, Vimentin, ROCK, Phosphorylation, Sphingosine 1-phosphate, Sphingosylphosphorylcholine, migration, $S1P_2$, S1PR2, Intermediate filament

INTRODUCTION

Sphingolipids are perhaps best known as building blocks of biological membranes, but they are also versatile signalling molecules. The sphingolipid sphingosine 1-phosphate (S1P) regulates many cancer-related processes, including proliferation, motility, survival, angiogenesis and inflammation. It is also considered as a cancer-promoting signalling factor, because overexpression of sphingosine kinase 1 (SK1, also known as SPHK1), the enzyme that produces S1P, is common in tumours and high SK1 expression also correlates with poor prognosis. Accordingly, S1P signalling is studied as a potential target for cancer therapy (Pyne and Pyne, 2010). Sphingosylphosphorylcholine (SPC) is another bioactive sphingolipid also present in plasma. Compared to S1P, its functions are less-well understood, but it does regulate many of the same cancer-related processes as S1P. Depending on the cell type, S1P and SPC have either similar or different effects, perhaps due to specificity for different receptors (Alewijnse and Michel, 2006; Nixon et al., 2008).

Whether S1P actually has a stimulatory or inhibitory effect on cancer cells depends on the context, indicating that sphingolipid signalling is actively processed to determine the outcome. This signal processing could be dependent upon receptor composition, as five G-protein-coupled receptors have been identified for S1P ($S1P_1$–$S1P_5$, also known as S1PR1–S1PR5) and these receptors preferentially couple to different downstream pathways with overlapping but also opposing functions (Adada et al., 2013; Meyer zu Heringdorf and Jakobs, 2007). S1P also has a number of direct intracellular targets (Alvarez et al., 2010; Hait et al., 2009), which participate in signal processing.

Among the identified targets for SPC signalling are the intermediate filament proteins, keratins 8 and 18 (K8 and K18), with site-specific phosphorylation being a key mediator of the SPC-induced effects on keratin network reorganisation and cell motility (Beil et al., 2003; Busch et al., 2012; Fois et al., 2013; Park et al., 2011). Another member of the intermediate filament family, vimentin, has well established roles in migratory signalling and processes, often acting in concert with K8/K18 (Hyder et al., 2011; Ivaska et al., 2007; Pallari and Eriksson, 2006). Interestingly, an early study indicated that S1P caused vimentin filament reorganisation (Sin et al., 1998). Furthermore, in the presence of S1P, vimentin forms complexes with FAK (also known as PTK2) and RACK1 (also known as GNB2L1) in invading endothelial cells, which regulates focal adhesion formation and cell adhesion (Dave et al., 2013).

Vimentin is well known as a marker of epithelial–mesenchymal transition (EMT; Ivaska, 2011). Vimentin expression is associated with metastatic ability and it is widely accepted to be important for migratory functions (Chung et al., 2013; Nieminen et al., 2006). One key way that vimentin regulates cell motility is through dynamic reorganisation of its constituent filament network, which is regulated by phosphorylation on the N-terminus (Hyder et al., 2008; Ivaska et al., 2007). Phosphorylation serves to stimulate depolymerisation and turnover of the network. Conversely, dephosphorylation can stimulate network assembly and inhibit turnover (Snider and Omary, 2014). Recent work has shown that vimentin filaments are inhibitory for lamellipodia formation and ruffling, but are necessary for cell movement. In fact, phosphorylation-mediated disassembly of the vimentin network at the cell periphery is a prerequisite for actin-dependent lamellipodia formation and is necessary for lamellipodia stability (Helfand et al., 2011). Vimentin phosphorylation is also important for integrin recycling and cell motility (Barberis et al., 2009; Ivaska et al., 2005) and might also regulate focal adhesion turnover (Svitkina et al.,

[1]Turku Centre for Biotechnology, University of Turku and Åbo Akademi University, POB 123, FIN-20521, Turku, Finland. [2]Department of Biosciences, Åbo Akademi University, Tykistökatu 6A, FI-20520, Turku, Finland. [3]Environmental Science Lab, Faculty of Pharmacy, Meijo University, Yagotoyama 150, Tempaku. Nagoya 468-8503, Japan. [4]Division of Biochemistry, Aichi Cancer Center Research Institute, Kanokoden, Chikusa-Ku, Nagoya 464-8681, Japan. [5]Department of Cellular Oncology, Graduate School of Medicine, Nagoya University, Showa-Ku, Nagoya 466-8550, Japan. [6]Minerva Foundation Institute for Medical Research, Biomedicum Helsinki, Tukholmankatu 8, 00290 Helsinki, Finland.
*These authors contributed equally to this work

‡Authors for correspondence (john.eriksson@abo.fi; ktornqvi@abo.fi)

Received 23 July 2014; Accepted 20 April 2015

Journal of Cell Science

Journal of Cell Science (2015) 128, 2057-2069 doi:10.1242/jcs.160341

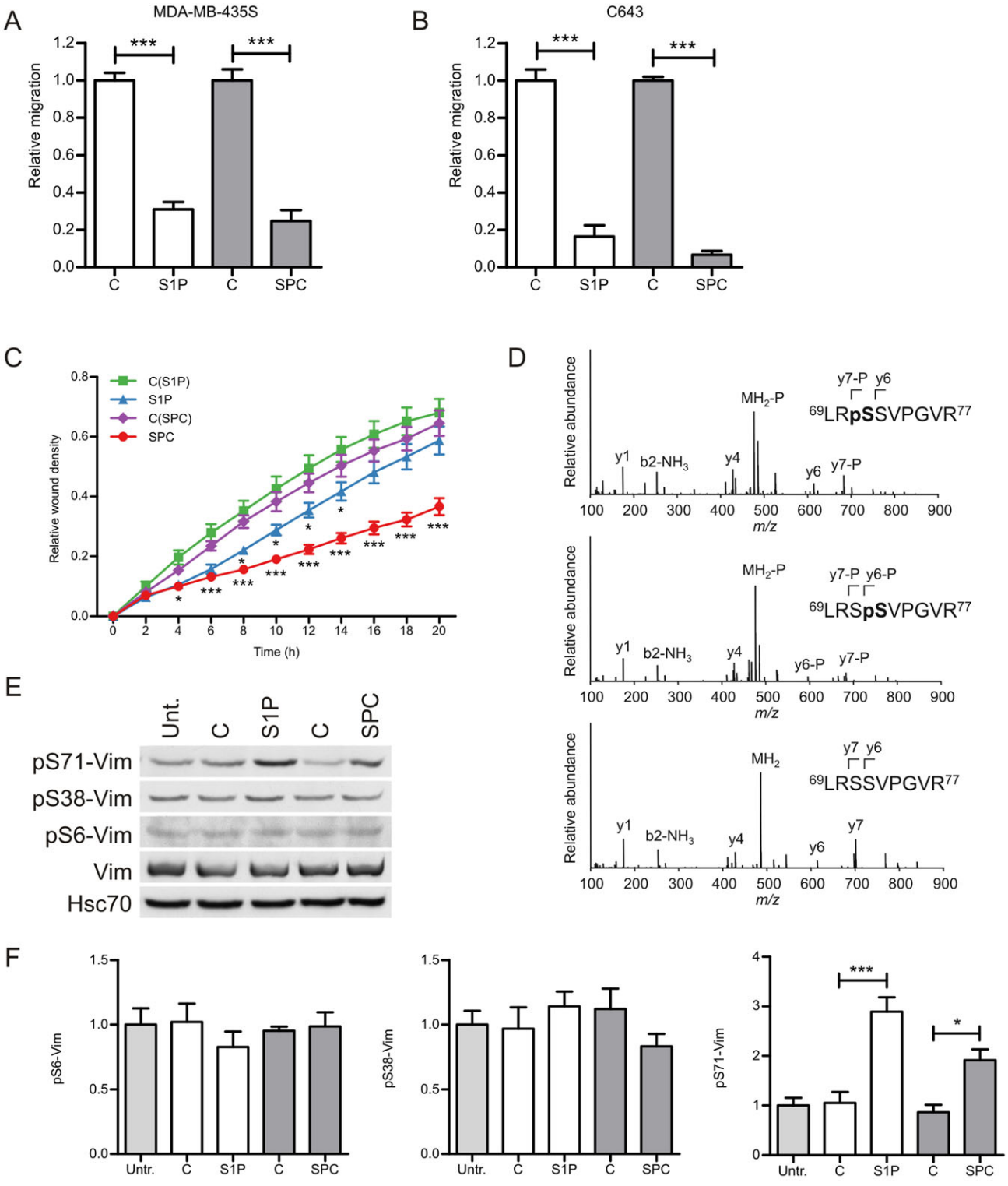

Fig. 1. See next page for legend.

1996) and integrin surface expression (Nieminen et al., 2006). Vimentin also functions as a signalling organiser. In the context of migration, vimentin has been shown to act as a scaffold for RhoA-binding kinase (Sin et al., 1998) and the vasodilator-stimulated phosphoprotein (VASP), thereby regulating VASP activation and targeting to focal adhesion (Lund et al., 2010).

Considering that vimentin has well established roles in cell migration and motility, and in light of its tentative association with S1P signalling, we wanted to determine whether vimentin could be a structural element that provides the functional context for sphingolipid signalling. In the present study, we show that S1P and SPC inhibit cancer cell migration, in concert with phosphorylation of vimentin on S71 (pS71) and reorganization of the vimentin filament network. The sphingolipid-dependency of the effects on vimentin was demonstrated by inhibition of the $S1P_2$ receptor or its downstream effector ROCK (for which there are two

Journal of Cell Science (2015) 128, 2057-2069 doi:10.1242/jcs.160341

Fig. 1. S1P and SPC inhibit migration and induce vimentin phosphorylation at S71. (A) Sphingolipid treatment dramatically inhibits chemotactic MDA-MB-435S cell migration. Cells were allowed to migrate in Boyden chambers towards 10% lipid-stripped serum and vehicle control (C), S1P (15 nM) or SPC (700 nM) for 16 h. Results are mean±s.e.m., n=6–7. (B) Sphingolipid treatment dramatically inhibits chemotactic C643 cell migration. Cells were allowed to migrate in Boyden chambers towards 10% lipid-stripped serum and vehicle control (C), S1P (100 nM) or SPC (10 µM) for 6 h. Results are mean±s.e.m., n=4–6. (C) Sphingolipid treatment impairs C643 scrape wound healing. Cells were grown to a monolayer. A scratch wound was made. Initial images were taken using the Incucyte ZOOM and the cells were treated with S1P (100 nM), SPC (10 µM) or their respective controls. The wounds were made prior to treatment because sphingolipid treatment causes a temporary rounding of the cells which would be detrimental for imaging of the initial wound. Wound closure was followed for 20 h and images were taken every hour. Relative wound density was calculated by the Incucyte ZOOM software and represents the density of the wound at the indicated time points compared to the initial wound. Graph shows quantification of relative wound density, mean±s.e.m., n=3. (D) LC-MS/MS analysis of a vimentin phosphorylation site induced by SPC and S1P in MDA-MB-435S cells. Cells were treated with vehicle control, S1P (100 nM, 30 min) or SPC (1 µM, 1 h). After in-gel tryptic digestion and TiO_2 phosphopeptide enrichment, a peptide $L^{69}RpSSVPGVR^{77}$ (pS71) was identified as a vimentin phosphopeptide induced by both the sphingolipids (refer to supplementary material Fig. S1; supplementary material Table S1). To validate the phosphorylation site, MS/MS spectra of pS71, pS72 and the non-phosphorylated form of the peptide were comparatively interpreted. These peptides were observed in all the four samples (S1P, SPC and respective control samples), and representative MS/MS spectra are shown here. A neutral loss of phosphoric acid (-P) was observed at the phosphorylated serine residues. (E) Validation of vimentin S6, S38 and S71 phosphorylation induced by sphingolipid treatment in MDA-MB-435S cells. Western blot analysis and quantification using phosphosite-specific antibodies shows that only phosphorylation of vimentin S71 (pS71-Vim) is significantly induced following treatment of MDA-MB-435S cells with S1P (100 nM, 30 min) or with SPC (10 µM, 1 h). (F) The graphs show quantification of the results in E (mean±s.e.m., n=3–5). *P<0.05, ***P<0.001 between sphingolipid treatment and vehicle control (C) [Student's t-test (A,B), two-way ANOVA with Bonferroni's post-hoc test (C) or one-way ANOVA with Bonferroni's post-hoc test (F)].

isoforms, ROCK1 and ROCK2). Importantly, we found that the S1P- and SPC-induced inhibition of cancer cell migration is dependent on vimentin S71 phosphorylation, indicating that vimentin serves as a key mediator when sphingolipid signalling regulates cell migration.

RESULTS

Sphingolipids inhibit cell migration in MDA-MB-435S and C643 cells

Whether the effect of S1P and SPC on migration is inhibitory or stimulatory is context dependent. We found that S1P and SPC inhibited migration of the cancer cell line MDA-MB-435S in the chemotactic Boyden chamber model (Fig. 1A). Previously we have shown that treatment of another cancer cell line (C643) with S1P inhibits their migration in Boyden chambers (Asghar et al., 2012). We repeated the experiment and observed that SPC also had an inhibitory effect (Fig. 1B). Wound-healing experiments were performed with C643 cells to test the effect of the sphingolipids using another migration model and we observed that both S1P and SPC inhibited wound healing (Fig. 1C), although SPC appeared to have a greater inhibitory effect on wound closure.

Sphingolipids induce phosphorylation of vimentin on S71

Given that both S1P and SPC inhibit migration in our cell models (Fig. 1A–C), and it is well known that vimentin regulates cell motility (Chung et al., 2013), we hypothesized that these lipids might regulate vimentin. Phosphorylation is one of the primary post-translational modifications (PTM) regulating vimentin organisation (Hyder et al., 2008; Izawa and Inagaki, 2006). Vimentin has more than 20 phosphorylation sites of which at least 11 are physiologically relevant *in vivo* (Eriksson et al., 2004). Therefore, we performed mass spectrometry to identify whether sphingolipids alter vimentin phosphorylation in MDA-MB-435S cells (supplementary material Table S1). Based on the mass spectrometry screen, we observed that both S1P and SPC treatment increased phosphorylation of vimentin especially at S71 (Fig. 1D; supplementary material Fig. S1). S24 or S25, S38 and S41 were also identified as phosphorylation targets upon S1P or SPC treatment (supplementary material Table S1). The S71 phosphosite was chosen for further study, for three reasons: (1) sphingolipids are known to regulate ROCK activity, (2) ROCK is involved in cell migration (Amano et al., 2010; Inada et al., 1999) and (3) S71 on vimentin has been implicated as a target for ROCK (Goto et al., 1998; Inada et al., 1999). The mass spectrometry results were validated by western blotting using antibodies specific for phosphorylated S38 and S71 (Fig. 1E,F; Nakamura et al., 2000). S6 has a role in motility and was also included (Barberis et al., 2009; Ivaska et al., 2005; Kim et al., 2010), although mass spectrometry did not identify it. These results demonstrated that S71 is the primary vimentin phosphorylation site induced by S1P and SPC.

Sphingolipids induce vimentin reorganisation

Given that phosphorylation is a potent regulator of vimentin network organisation, we investigated how sphingolipid treatment affected the vimentin network. Immunofluorescence labelling revealed that S1P and SPC caused a reorganisation of the vimentin cytoskeleton from an orderly network that was distributed throughout the cytoplasm, to one that was more concentrated in the perinuclear regions (Fig. 2A; supplementary material Fig. S1C). This was evident even though the sphingolipids also caused cell rounding. The vimentin filament network became less organised in the case of SPC treatment and the filaments retracted into the perinuclear space with S1P treatment (Fig. 2A). To quantify the effect of sphingolipid treatment on cell shape we measured the perimeter length and volume of treated cells. We found that both S1P and SPC caused a small but significant decrease in the cell perimeter length and S1P also decreased cell volume (Fig. 2B,C). When we investigated the effects of sphingolipids on mouse embryonic fibroblasts (MEFs), S1P and SPC treatment did not cause vimentin reorganisation or cell morphology changes (supplementary material Fig. S1D).

Vimentin assembly is a dynamic process whereby vimentin filaments are organised from monomers that assemble into unit length filament (ULF) precursors. The ULFs then self-assemble into filaments. To further elucidate the effect of S1P and SPC on vimentin organisation and dynamics, we performed fluorescence recovery after photobleaching (FRAP) experiments in MDA-MB-435S cells to monitor assembly and turnover of the vimentin network (supplementary material Fig. S2; supplementary material Movies 1,2). FRAP results show that S1P treatment causes a decrease in the turnover of vimentin filaments as indicated by the fluorescence recovery half-time ($t_{½}$), which is 9.9 min for S1P-treated MDA-MB-435S cells compared to $t_{½}$ of 4.7 min for control cells (*P=0.0348, n=12–17, imaging during 0–60 min after S1P treatment). This is also shown as typical recovery curves (supplementary material Fig. S2). The results support our observations shown in Fig. 2A. The recovery half time of the control is similar to what has been observed previously (Yoon et al., 1998). A recent article has shown that ROCK inhibits the transport of vimentin ULFs along microtubules (Robert et al., 2014). Given that the sphingolipids are known to induce ROCK activity, the

Journal of Cell Science (2015) 128, 2057-2069 doi:10.1242/jcs.160341

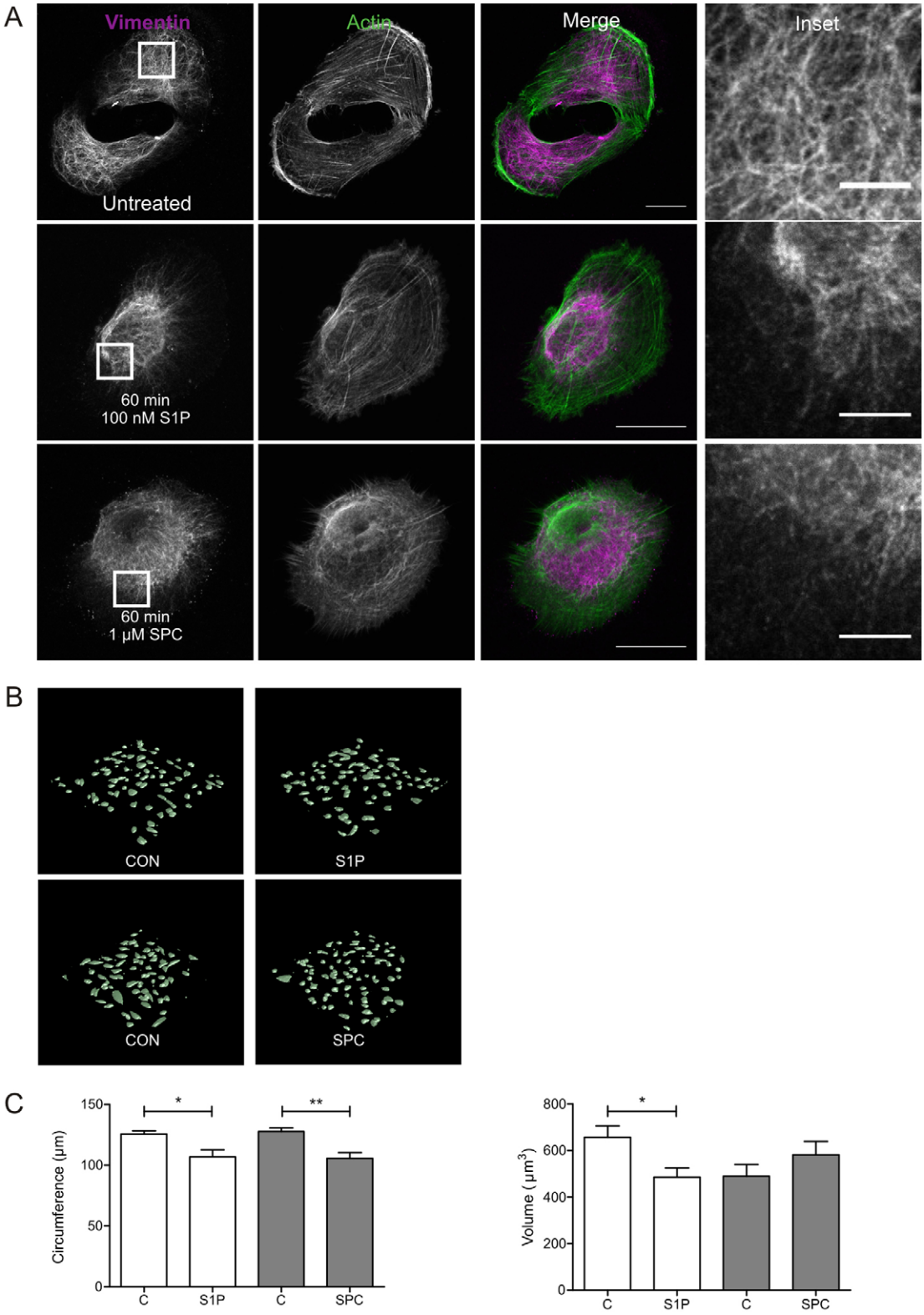

Fig. 2. Sphingolipids S1P and SPC cause vimentin reorganisation. (A) Representative immunofluorescence images showing that sphingolipid treatment causes cell rounding and reorganisation of the vimentin and actin cytoskeleton in C643 cells. Cells were co-labelled for vimentin (magenta) and actin using fluorescently conjugated phalloidin (green). White squares on the vimentin images indicate the area of the magnified images shown in the inset. Scale bars: 20 µm (main images); 5 µm (inset). (B) 3D projections of confocal stacks of whole-cell-stained (CFSE) C643 cells show rounding effects of S1P and SPC treatment. Cells grown on coverslips were labelled with CFSE and treated with vehicle control (C), S1P (100 nM) or SPC (1 µM) for 30 min. Cells were fixed and CFSE stain was imaged with confocal microscope. 3D surface rendering projections were created with BioImageXD. (C) S1P and SPC decrease the cell perimeter and S1P decreases cell volume. The 3D image stacks described in B were segmented to identify whole cells using BioImageXD. Cell volumes were measured from six stacks per treatment in two separate experiments (minimum 300 cells per treatment). The length of the cell perimeter was measured with CellProfiler. **P*<0.05, ***P*<0.01 (Student's *t*-test).

Journal of Cell Science (2015) 128, 2057-2069 doi:10.1242/jcs.160341

decrease in vimentin turnover in the FRAP experiment could be a result of decreased ULF transport.

Kinetics of sphingolipid-induced vimentin S71 phosphorylation

Given the observed dramatic induction of phosphorylation, we wanted to analyse the kinetics of the phosphorylation to see how rapidly it was induced and how long it persisted. Analysis of vimentin S71 phosphorylation (pS71-vimentin) kinetics indicated induction within 10 min by S1P in both MDA-MB-435S and C643 cells. This gradually decreased over the course of 4 h (Fig. 3). SPC-induced pS71 in both MDA-MB-435S and C643 cells was also observed within 10 min. However, the kinetics was slower and more sustained compared to S1P (Fig. 3).

Sphingolipids regulate vimentin organisation and cell migration through $S1P_2$

There are five specific S1P receptors ($S1P_1$–$S1P_5$), of which $S1P_1$–$S1P_3$ are ubiquitous. $S1P_1$ and $S1P_3$ receptors are pro-migratory, whereas the $S1P_2$ receptor is usually anti-migratory (Adada et al., 2013; Meyer zu Heringdorf and Jakobs, 2007; Pyne and Pyne, 2010). We have previously shown that the $S1P_2$ receptor is expressed in C643 cells and that it mediates S1P-induced inhibition of migration (Asghar et al., 2012). Therefore, we hypothesised that S1P and SPC might regulate vimentin through $S1P_2$. To study this, we silenced the $S1P_2$ receptor with small interfering RNA (siRNA), achieving ∼65% knockdown at the mRNA level (Fig. 4A). Additionally, we utilised the $S1P_2$ receptor inhibitor JTE013 (Fig. 4B; supplementary material Fig. S3A). Both treatments inhibited sphingolipid-induced pS71-vimentin. JTE013 also prevented sphingolipid-induced vimentin reorganisation and cell rounding (Fig. 4C). Vector plots from single-cell-tracking experiments revealed that both S1P and SPC restricted the motility of MDA-MB-435S cells (Fig. 4D,E). In particular, the velocity of single cells was affected by sphingolipid treatment (Fig. 4E). Interestingly, MDA-MB-435S cells exhibited a range of velocities during single cell tracking, and S1P treatment restricted the velocities of MDA-MB-435S cells to between 0.02–0.2 µm/min (Fig. 4E). Taken together, this data identifies $S1P_2$ as the primary receptor responsible for transducing the S1P and SPC cellular effects in our cell models.

Sphingolipids regulate vimentin organisation and cell migration through ROCK

$S1P_2$ inhibits migration through a signalling cascade including $G_{12/13}$, Rho and ROCK (Lepley et al., 2005). ROCK is known to phosphorylate vimentin on S71 (Goto et al., 1998). Notably, when Sin et al. (Sin et al., 1998) studied Rho/ROCK-induced vimentin phosphorylation and organisation change in HeLa cells they used S1P (1 µM) as a Rho activator and saw a S1P-induced collapse of the vimentin network. Therefore, we hypothesised that S1P and SPC may regulate vimentin phosphorylation and organisation via the $S1P_2$/Rho/ROCK pathway in our model systems. We have already confirmed (Fig. 4) that $S1P_2$ transduces S1P and SPC signals in

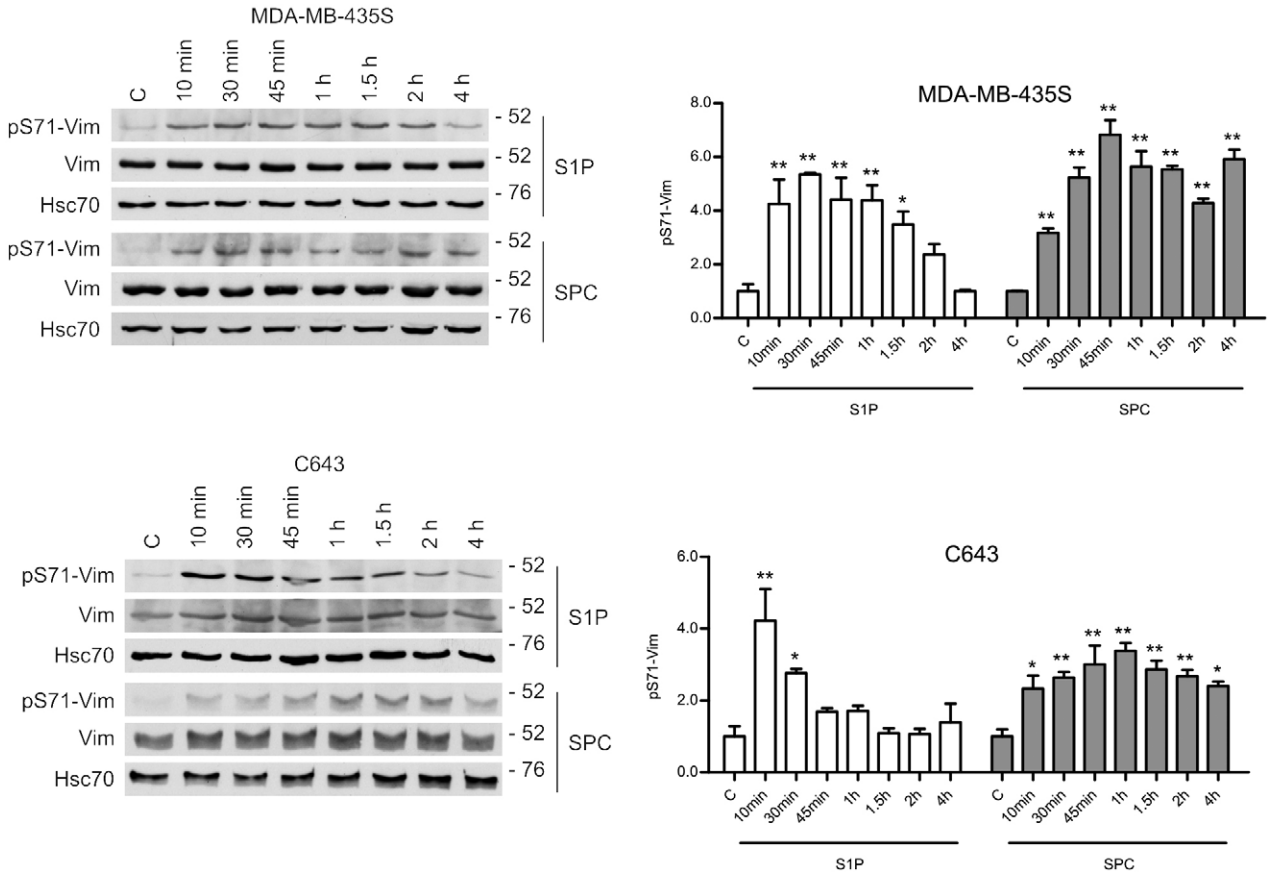

Fig. 3. Kinetics of S1P- and SPC-induced vimentin S71 phosphorylation. MDA-MB-435S and C643 cells were treated with S1P (100 nM) or SPC (10 µM) for the times indicated and then the phosphorylation of vimentin S71 was analysed by western blotting. Results are mean±s.e.m., n=3. *P<0.05, **P<0.01 between sphingolipid treatment and vehicle control (C) (one-way ANOVA with Dunnett's post-hoc test).

Journal of Cell Science (2015) 128, 2057-2069 doi:10.1242/jcs.160341

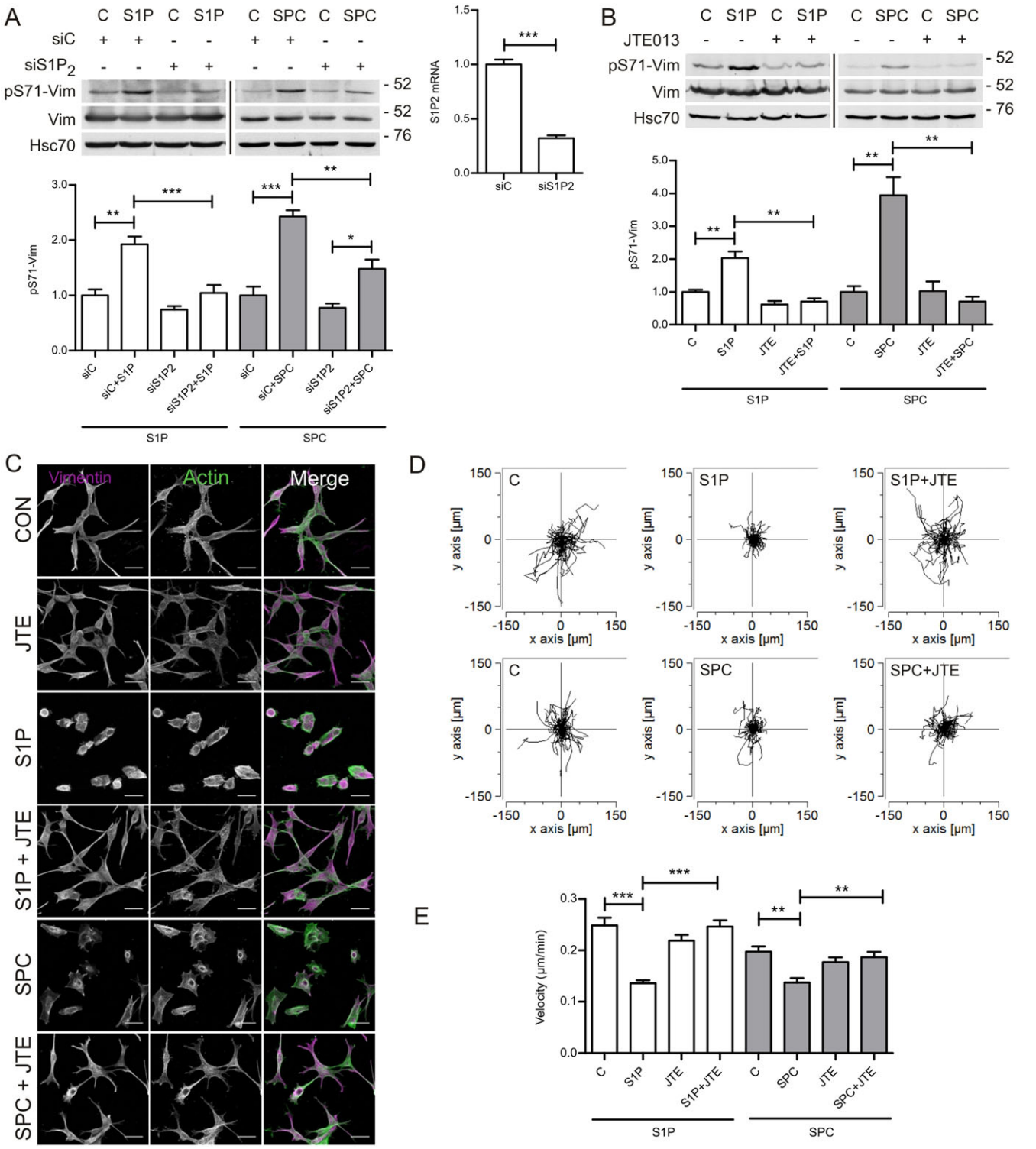

Fig. 4. S1P and SPC act through $S1P_2$ to phosphorylate vimentin and inhibit cell migration. (A) Knockdown of $S1P_2$ prevents S1P- and SPC-induced vimentin S71 phosphorylation. MDA-MB-435S cells transfected with siControl or si$S1P_2$ were treated with vehicle control (C), S1P (100 nM, 10 min) or SPC (10 μM, 1 h). Results are mean±s.e.m., *n*=5. (B) Inhibition of $S1P_2$ prevents S1P- and SPC-induced vimentin S71 phosphorylation (pS71-Vim). MDA-MB-435S cells were pre-treated with the $S1P_2$ inhibitor JTE013 (10 μM, 1 h) and then treated with vehicle control (C), S1P (100 nM, 10 min) or SPC (10 μM, 1 h). Results are mean±s.e.m., *n*=3. (C) Representative immunofluorescence images showing $S1P_2$ inhibition with JTE013 prevents S1P and SPC induced cell rounding and reorganisation of vimentin in MDA-MB-435S cells. Cells were pre-treated with JTE013 (10 μM, 1 h) as indicated before treatment with vehicle control (CON), S1P (100 nM, 30 min) or SPC (1 μM, 1 h). Cells were co-labelled for vimentin (magenta) and actin using fluorescently conjugated phalloidin (green). Scale bars: 20 μm. (D) Single-cell tracking shows that S1P and SPC inhibits the movement of MDA-MB-435S cells which is rescued by $S1P_2$ inhibition. Cells were treated with vehicle control (C), S1P (100 nM) or SPC (1 μM) and JTE013 (10 μM) combined (S1P or SPC +JTE; plots for JTE alone not shown). Plots show the tracks of 60 randomly selected cells from three independent experiments. Cells were tracked for 6 h and wide-field images were obtained every 45 min. The intersection of the *x*- and *y*-axis is the starting point for each cell. (E) S1P and SPC inhibit velocity of MDA-MB-435S movement and this is rescued by $S1P_2$ inhibition. Graph shows the velocity of the cells tracked in D. **P*<0.05, ***P*<0.01, ****P*<0.001 (one-way ANOVA with Bonferroni's post-hoc test (A,B,E) or Student's *t*-test (A)).

Journal of Cell Science (2015) 128, 2057-2069 doi:10.1242/jcs.160341

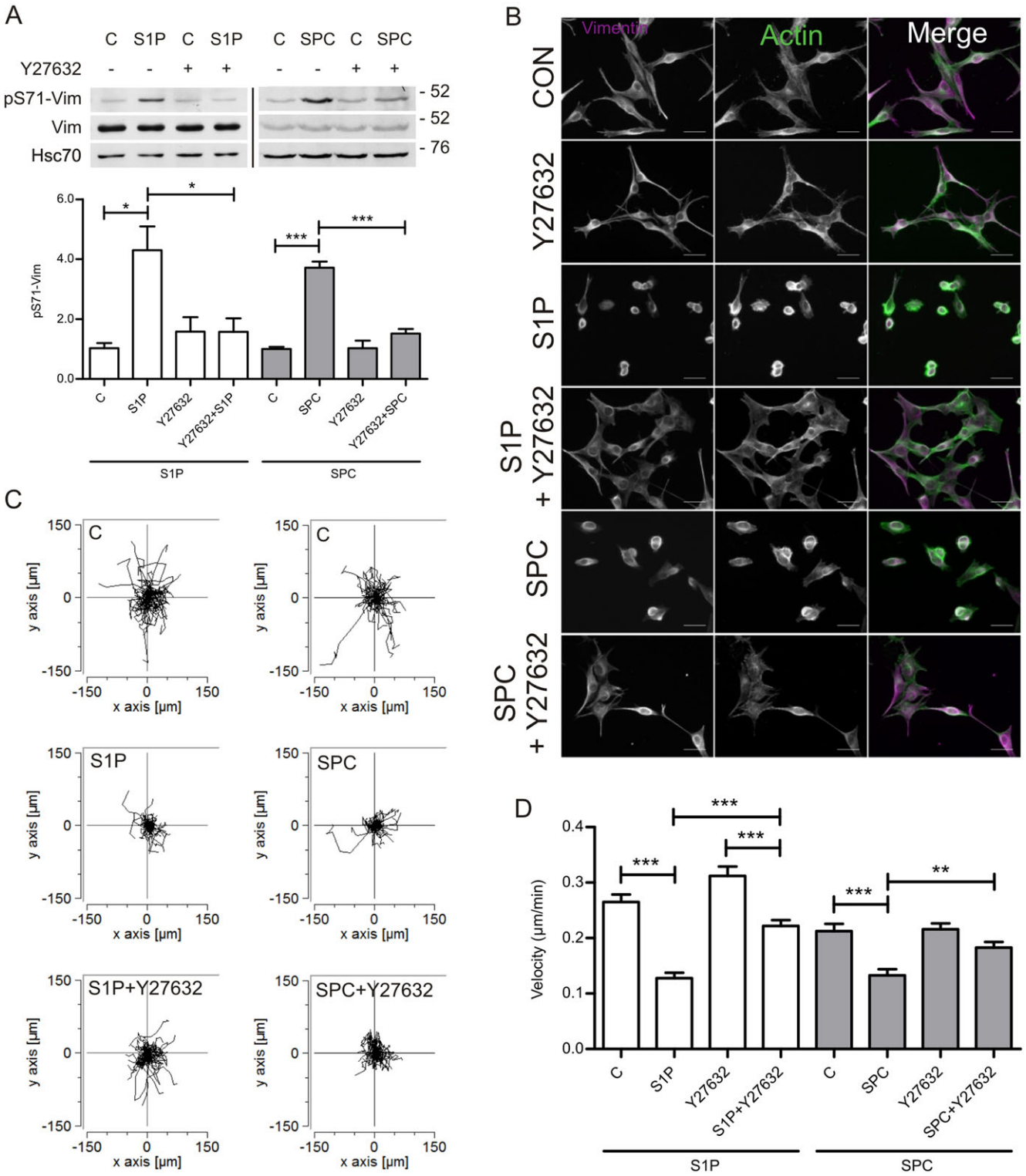

Fig. 5. S1P and SPC act through ROCK to induce vimentin phosphorylation at S71, cause vimentin reorganisation and inhibit cell movement. (A) Inhibition of ROCK prevents S1P- and SPC-induced vimentin S71 phosphorylation (pS71-Vim). MDA-MB-435S cells were pre-treated with ROCK inhibitor Y27632 (10 µM, 1 h) and treated with vehicle control (C), S1P (100 nM, 10 min) or SPC (10 µM, 1 h). Whole-cell lysates were prepared and used for western blotting. Results are mean±s.e.m., *n*=3. (B) ROCK inhibition with Y27632 prevents the S1P- and SPC-induced cell rounding and perinuclear reorganisation of vimentin in MDA-MB-435S cells. Cells were pre-treated with Y27632 (10 µM, overnight) as indicated before treatment with vehicle control (C), S1P (100 nM, 30 min) or SPC (1 µM, 1 h). Cells were co-labelled for vimentin (magenta) and actin using fluorescently-conjugated phalloidin (green). Scale bars: 20 µm. (C) S1P and SPC inhibit the movement of MDA-MB-435S cells which is rescued by ROCK inhibition. Cells were treated with vehicle control (C), S1P (100 nM) or SPC (1 µM) and Y27632 (10 µM) combined (S1P or SPC+Y2763, plots for Y27632 alone not shown). Plots show the tracks of 60 randomly selected cells from three independent experiments. Cells were tracked for 6 h and wide-field images were obtained every 45 min using Cell-IQ. The intersection of the *x*- and *y*-axis is the starting point for each cell. (D) S1P and SPC inhibit velocity of MDA-MB-435S and this is attenuated by ROCK inhibition. Graph shows the velocity of the cells tracked in C). **P*<0.05, ***P*<0.01, ****P*<0.001 (one-way ANOVA with Bonferroni's post-hoc test).

Journal of Cell Science

Journal of Cell Science (2015) 128, 2057-2069 doi:10.1242/jcs.160341

MDA-MB-435S and C643 cells. To study the involvement of ROCK in this pathway, we used the well-established ROCK inhibitor Y27632. Inhibition of ROCK prevented sphingolipid-induced pS71-vimentin (Fig. 5A; supplementary material Fig. S3B). Immunofluorescence labelling demonstrated that ROCK inhibition by Y27632 also rescued the S1P- and SPC-induced effects on cell morphology and vimentin organisation (Fig. 5B). Tracking of single cells revealed that ROCK inhibition attenuated sphingolipid-induced inhibition of cell motility in MDA-MB-435S cells (Fig. 5C,D), in particular velocity (Fig. 5D).

To further investigate this feature, we performed wound-healing experiments using C643 cells in which we analysed the overall wound closure, as well as the migration of individual cells into the wound following sphingolipid treatment (supplementary material Fig. S3C–E). Vector plots clearly show that S1P treatment restricted the movement of cells from the edge of the wound and ROCK inhibition prevented this restriction to take place (supplementary material Fig. S3D). Not only was the velocity of the cells reduced, the ability of the cells to migrate in a persistent direction was also impeded (supplementary material Fig. S3E). This is demonstrated by the forward migration index, a measure of chemotactic effect (supplementary material Fig. S3E). S1P treatment significantly reduced the efficiency of chemotaxis in a ROCK-dependent manner. Our data strongly suggests that ROCK mediates S71-vimentin phosphorylation, with consequences for migration. This is supported by the existence of a ROCK consensus site at S71, VRLRSSVPG (underlined; Loirand et al., 2006; Shi et al., 2007). This is in line with results from numerous past studies demonstrating that ROCK mediates pS71-vimentin formation (Bauer et al., 2012; Goto et al., 1998; Inada et al., 1999; Lei et al., 2013; Nakamura et al., 2000; Yokoyama et al., 2005). None of these studies show a direct ROCK–vimentin interaction in co-immunoprecipitation experiments, which we also were not able to consistently observe. This suggests that the ROCK–vimentin interaction, like many kinase–substrate interactions, is very transient making it problematic to capture reliably with biochemical assays.

S1P and SPC regulate cell migration through vimentin

To determine whether vimentin is important for sphingolipid-dependent inhibition of migration we employed wild-type (WT) vimentin and vimentin-knockout (KO) MEFs. First, we determined that the vimentin WT MEFs do respond to sphingolipids and saw that both S1P and SPC-induced pS71-vimentin (Fig. 6A). We then performed a Boyden chamber migration experiment on both vimentin WT and KO MEFs with and without sphingolipid treatment (Fig. 6B,C). This showed that, like the C643 and MDA-MB-435S cells, vimentin WT MEF migration is inhibited by sphingolipid treatment. Vimentin KO MEFs, however, had a negligible response to sphingolipid treatment, indicating that vimentin is important for the inhibitory effect of the sphingolipids on migration (Fig. 6B).

S1P and SPC regulate cancer cell migration through vimentin S71 phosphorylation

The consistent interrelationship between S1P and SPC signalling, pS71-vimentin and effects on migration, strongly pointed towards a causal relationship between all of these events. To verify whether the sphingolipid-induced pS71-vimentin was indeed the prime cause for the observed inhibition of migration, we utilised a plasmid expressing an mCherry-tagged phosphorylation-deficient S71A mutation of vimentin (S71A-Vim) (Pan et al., 2011). In agreement with the postulated causal relationship, based on the accumulated data, the inhibitory effect of S1P and SPC on chemotactic migration was effectively nullified in the S71A-Vim-expressing cells (Fig. 6D). Western blotting and immunofluorescence were used to check cells for mCherry–vimentin expression (Fig. 6E–G). Transfected cells expressed mCherry–vimentin at a level that was approximately half of the expression level of endogenous vimentin (Fig. 6E). Quantification of the number of mCherry–vimentin-expressing cells confirmed that mCherry–vimentin-WT and -S71A were expressed in ∼50% of the cells (Fig. 6G). Interestingly, it appeared that expression of S71A by itself exhibited elevated cell motility compared to WT vimentin, suggesting that basal levels of pS71-vimentin restricts cell motility to some extent. This is highly plausible, as S71 is indeed among those sites that are constitutively phosphorylated without further stimulation (Eriksson et al., 2004). The results in MEFs and MDA-MB-435S cells demonstrate that not only vimentin by itself is important, but that the event of sphingolipid-induced pS71-vimentin, which is key to the sphingolipid-induced inhibition of chemotactic migration of these cells. Taken together, our study demonstrates that S1P and SPC have the capacity to strongly inhibit cell motility through $S1P_2$- and ROCK-mediated phosphorylation of vimentin at S71 (Fig. 7).

DISCUSSION

Although both vimentin and S1P are well-known regulators of cellular migration, invasion and subsequently metastasis, and have also been studied as potential cancer therapy targets (Pyne and Pyne, 2010; Satelli and Li, 2011), the relationship between the two has not been extensively studied. In addition, even though vimentin S71 is a known substrate of ROCK, a connection to cell motility has not been previously shown. In this study, we show that activation of the $S1P_2$–ROCK pathway by S1P or SPC inhibits cancer cell migration by inducing ROCK-mediated pS71-vimentin (Fig. 7). A reorganisation of the vimentin network might play a role in this anti-migratory effect. Little is known about the involvement of S1P and SPC with the intermediate filament cytoskeleton. Most relevant to this work is an early study showing that S1P simultaneously affects both ROCK and vimentin network organisation (Sin et al., 1998). Although SPC has not, to our knowledge, been previously linked to vimentin function, it has been shown to increase elasticity and migration of pancreatic and gastric cancer cells through phosphorylation and re-organisation of the intermediate filament protein, keratin (Beil et al., 2003; Busch et al., 2012).

In this study, we conducted all experiments with both S1P and SPC to see whether we could see differences in terms of vimentin regulation by these two lipids. Although S1P has been extensively studied, SPC is still a somewhat enigmatic signalling lipid. Studies comparing S1P and SPC have shown that they have both similar and differing effects depending on the context. Because SPC is a low-affinity agonist for S1P receptors it is tempting to explain the similar functions of S1P and SPC as being mediated by S1P receptor activation, whereas differing effects might involve activation of other receptors by SPC (Alewijnse and Michel, 2006; Nixon et al., 2008). In our case, we saw little difference between the effects of S1P and SPC on vimentin reorganisation (Fig. 2A). The only notable difference between S1P and SPC in this study was in the kinetics of S71-vimentin phosphorylation (Fig. 3). This might arise from differences in affinity for and activation of the $S1P_2$ receptor by these lipids. Alternatively, it could be due to S1P-receptor-independent effects of SPC, for example, the potential SPC receptors OGR1 and GPR4 also couple to $G_{12/13}$–Rho (Li et al., 2013; Tobo et al., 2007). The induction of pS71-vimentin in C643 cells was comparatively weaker than in MDA-MB-435S cells

Journal of Cell Science (2015) 128, 2057-2069 doi:10.1242/jcs.160341

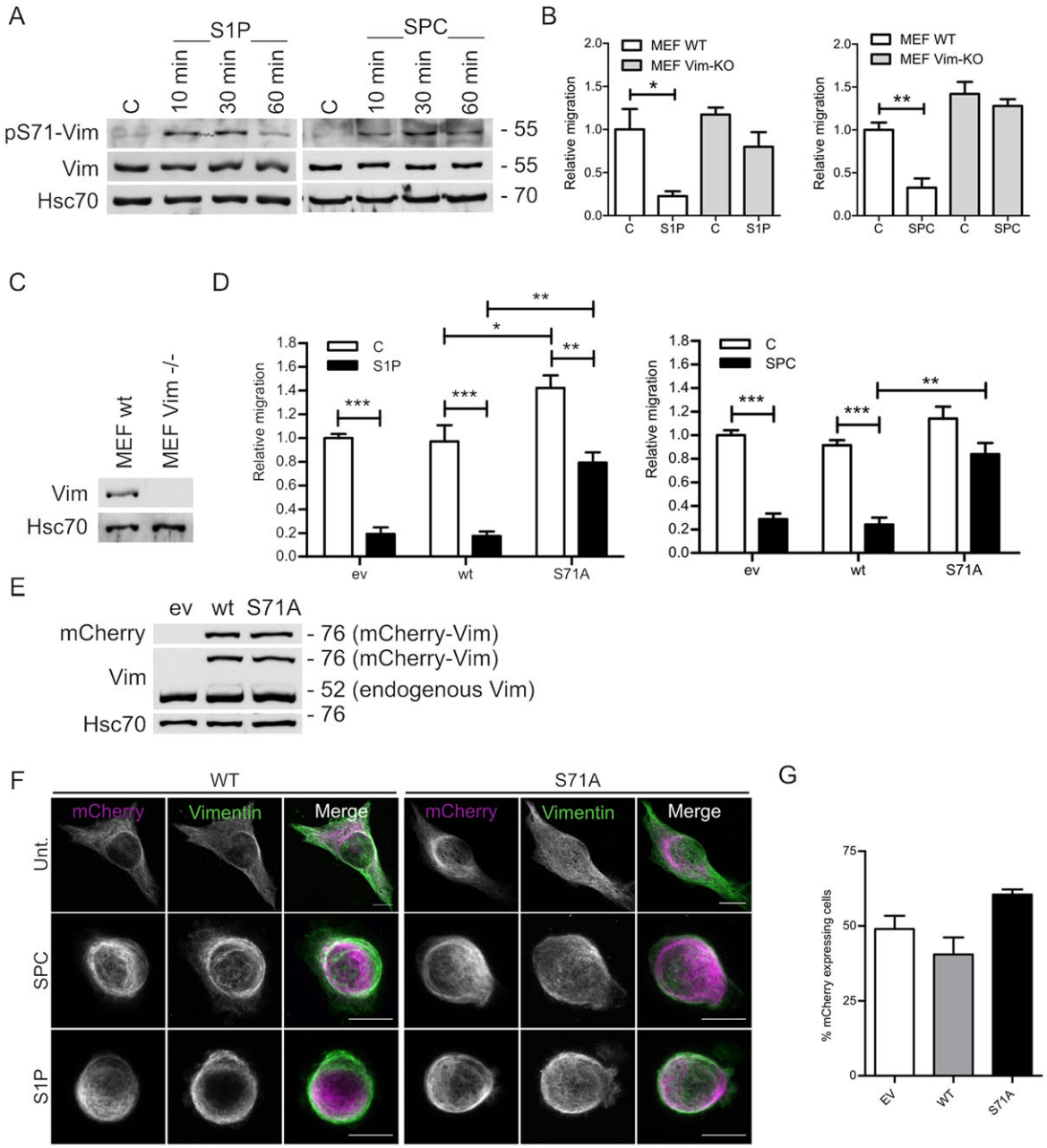

Fig. 6. Vimentin is important for the inhibitory effects of sphingolipids on cell migration. (A) Sphingolipids induce vimentin S71 phosphorylation (pS71-Vim) in WT MEFs. Cells were treated with S1P (100 nM) or SPC (10 µM) for the times indicated and phosphorylation of vimentin S71 was analysed by western blotting. Images shown are representative of three separate experiments. (B) Sphingolipid treatment inhibits chemotactic migration in WT MEFs but not in vimentin KO MEFs. Cells were allowed to migrate in Boyden chambers towards 10% lipid-stripped serum and vehicle control (C), S1P (10 nM) or SPC (1 µM). Results are mean±s.e.m., *n*=5. (C) Western blot to show vimentin levels in the vimentin WT and KO MEFs. (D) Expression of the unphosphorylatable S71A vimentin mutant in MDA-MB-435S cells attenuates the inhibitory effect of S1P and SPC on chemotactic cell migration. Cells were double transfected with mCherry–vimentin plasmids and migration experiments were performed as described in Fig. 1A. Results are mean±s.e.m., *n*=3. (E) Western blot to show the representative protein levels of mCherry–vimentin empty vector (EV), mCherry–vimentin WT and the unphosphorylatable mCherry–vimentin S71A mutant (S71A) compared to the endogenous vimentin levels in MDA-MB-435S cells. (F) Representative immunofluorescence images of the cells expressing the vectors described in E in MDA-MB-435S cells. Co-labelling with fluorescently conjugated phalloidin was used to indicate cell shape. Scale bars: 20 µm. (G) Graphs showing the percentage of transfected cells for each of the vectors. **P*<0.05, ***P*<0.01, ****P*<0.001 (one-way ANOVA with Bonferroni's post-hoc test).

even though the amount of $S1P_2$ is relatively similar in the two cell lines (supplementary material Fig. S4A). This might be because of differences in expression of signalling molecules downstream of the receptor.

We found that the sphingolipids S1P and SPC stimulate pS71-vimentin and that this event is responsible for the sphingolipid-induced inhibition of chemotactic cell migration (Fig. 6D). Wound healing experiments in which we analysed overall wound closure, as well as the migration of individual cells into the wound, showed that there was significantly reduced chemotaxis following S1P treatment (supplementary material Fig. S3C–E). The role of vimentin in cell motility has been well demonstrated previously. Merely the presence of vimentin has been shown to promote cell motility (Chung et al., 2013). A recent hypothesis suggests that vimentin maintains the

Journal of Cell Science (2015) 128, 2057-2069 doi:10.1242/jcs.160341

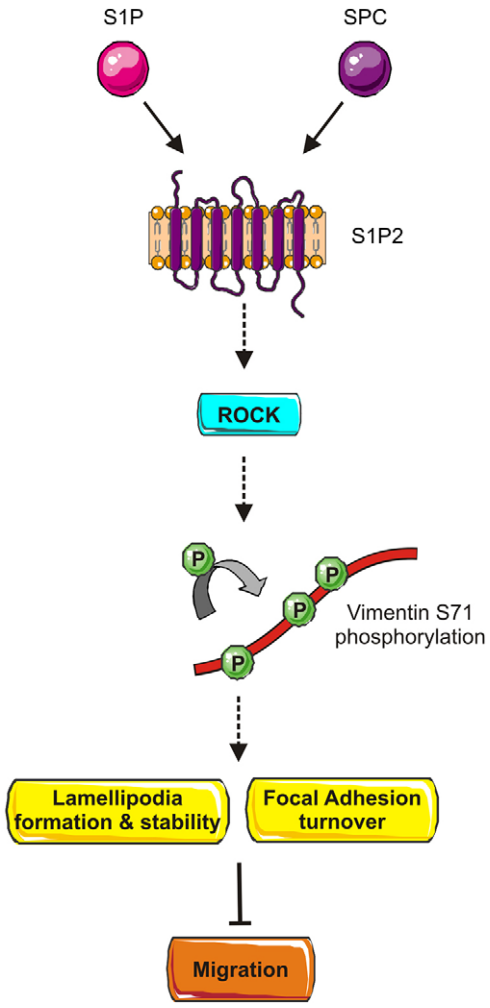

Fig. 7. Sphingolipids have the capacity to regulate migration by activation of $S1P_2$ and ROCK-mediated vimentin S71 phosphorylation. See text for more details.

directionality of a cell that has already committed to migrate (Chernoivanenko et al., 2013). Vimentin disassembly in targeted regions of the cell induces membrane ruffling and stimulates cells to change migration direction. Quantitative analysis has shown that the protein levels and the organisation of vimentin is also correlated with cell shape and migratory ability (Mendez et al., 2010). Previous studies have suggested that vimentin is associated with chemotaxis regulation. Fibroblasts derived from vimentin KO mice have chemotactic migration defects and defects in wound healing (Eckes et al., 1998; Eckes et al., 2000); this was attributed to improper focal adhesion organisation and sensing of chemotactic signals that affect directed cell migration (Eckes et al., 1998). In light of our results, we suggest that pS71-vimentin is important for chemotaxis. This might be because vimentin is important for cell motility, with a role in organising receptor molecules on the cell membrane and in the cellular localisation of adhesion-associated molecules and migration-regulating kinases (Hyder et al., 2011; Nieminen et al., 2006; Pallari and Eriksson, 2006; Sin et al., 1998). The exact role of vimentin phosphorylation in these processes remains to be determined.

The rescue experiments introducing the phosphorylation-deficient S71A mutant demonstrate that S71 phosphorylation contributes to cell motility. However, when our cell models were treated with S1P and SPC they tend to round up regardless of the expression of S71A. Furthermore, although S1P and SPC both induce pS71-vimentin in WT MEFs and inhibit migration of these cells, they do not induce any rounding of these cells (supplementary material Fig. S1D). Thus, the cell morphology effects caused by the sphingolipids in MDA-MB-435S and C643 cells are likely to be independent of pS71-vimentin and not directly coupled to the anti-migratory effect.

Agents targeted against SK1, S1P and the S1P receptors are being developed as cancer drugs and understandably so. SK1 is overexpressed in a variety of cancers, its expression correlates with malignancy and cancer cells have been shown to have a non-oncogene addiction to SK1 (Pyne and Pyne, 2010). The sphingolipid rheostat is a well-established model where S1P promotes survival, whereas its precursors ceramide and sphingosine increase apoptosis (Pyne and Pyne, 2010). However, effects of both S1P and SPC are very much cell specific. The $S1P_2$ receptor is an anti-tumorigenic factor because it inhibits both migration and proliferation; however, even this receptor has a pro-cancer function in some situations (Adada et al., 2013). Considering the work by ourselves and others on the influence of S1P on cell motility, care needs to be taken with regard to use of SK inhibitors because the actions of S1P clearly depend not only on the sphingolipid receptor profile of the cell type, but also on the transformation stage of the cancer. Given that tumours are highly heterogeneous, one can envisage that although SK1 inhibitors might have the desired anti-tumorigenic effect in some parts of the cancer, there may also be pro-tumorigenic effects. All in all, sphingolipid signalling is highly context-dependent and our study shows that targeting S1P in cancer might also have adverse effects. Furthermore, in the absence of S1P, SPC might still activate the same signalling cascades.

In the context of previous results regarding SPC regulation of keratin phosphorylation, our results also indicate that sphingolipids have a role in regulating intermediate filament organisation with consequences for cell motility. There are, however, notable differences. The first study on SPC and keratins in fact showed that SPC-induced keratin reorganisation promoted cell motility (Beil et al., 2003). This is most likely due to differences in S1P receptor activation and downstream signalling, cell type differences and the different roles between these groups of intermediate filaments. Keratins and vimentin exhibit very different cell and tissue expression patterns both during homeostasis and pathology, such as in cancer. Keratins are typically expressed at early stages of EMT. As EMT progresses, keratin expression decreases and vimentin is upregulated. It is interesting to consider how the two intermediate filament family members, vimentin and keratins, which are expressed at different stages of malignant transformation, are regulated in a differential manner by the same signalling molecules, with opposing effects on cell motility. These observations could be in keeping with the assumed differences in the roles of keratins and vimentin, respectively, the former being characteristic for rather stationary cells and the latter being specific for motile cells. Neither C643 nor MDA-MB-435S cells express keratins and their desmin expression is weak (supplementary material Fig. S4B,C; Alix-Panabières et al., 2009; Iyer et al., 2013; Sellappan et al., 2004). In this respect, we can be sure that the intermediate-filament-related sphingolipid effects in our cells are vimentin-dependent and not influenced by other intermediate filaments.

Although there is plentiful evidence for the involvement of vimentin in migratory functions, the exact molecular mechanisms underlying the effects of vimentin on the migratory machinery are not understood in detail. This study demonstrates that vimentin is important in migratory responses to external signalling stimuli, such

as those provided by the sphingolipids. Furthermore, we provide evidence that the effect of the sphingolipids through the $S1P_2$ receptor is a consequence of ROCK-mediated phosphorylation on vimentin S71, which in turn has consequences on the migratory functions of the cells.

MATERIALS AND METHODS

Cell culture

MDA-MB-435S human breast cancer cells were a kind gift from Hans-Peter Altevogt [German Cancer Research Center (DKFZ), Heidelberg, Germany] and C643 human anaplastic thyroid cancer cells from Nils-Erik Heldin (Karolinska Institutet, Stockholm, Sweden). Wild type (WT) and vimentin-knockout (KO) immortalised mouse embryonic fibroblast (MEF) cells were isolated by the Eriksson laboratory. MDA-MB-435S cells were cultured in RPMI 1640 (Lonza, Basel, Switzerland). C643 and MEF cells were cultured in DMEM (Sigma-Aldrich, St Louis, MO). Both media were supplemented with 10% fetal bovine serum (FBS), 1% L-glutamine and 1% penicillin-streptomycin (all from Life Technologies, Carlsbad, CA). RPMI was also supplemented with 1% non-essential amino acids (NEAA, Life Technologies). Cells were cultured in a humidified atmosphere containing 5% CO_2 at 37°C. Before sphingolipid treatments, cells were lipid-starved overnight in medium containing 5% lipid-stripped FBS. MEF cells were cultured for a maximum of ten passages.

Sphingolipid treatments were performed with D-*erythro*-sphingosine-1-phosphate (S1P; Enzo Life Sciences, Plymouth, PA) dissolved in HBSS buffer containing 4 mg/ml BSA, or D-*erythro*-sphingosylphosphorylcholine (SPC, Enzo Life Sciences) dissolved in 12% ethanol. For ROCK inhibition, cells were pre-treated with Y27632 (Calbiochem, San Diego, CA). For $S1P_2$ inhibition cells were pre-treated with the $S1P_2$ antagonist JTE013 (Tocris Biosciences, Ellisville, MO).

Transfections

Transfection of siRNA [control (siControl) or against $S1P_2$ ($siS1P_2$)] was performed by electroporation with the Gene Pulser Xcell Electroporation System (Bio-Rad, Hercules, CA). Cells and siRNA (2 µM) were mixed in Opti-MEM medium (Life Technologies) and pulsed at 220–240 V and 975 µF in a 0.4 cm cuvette. The siRNA sequences were 5′-CCUACAUCCCGAUCGAUGAUG(dTdT)-3′ for siControl (Berra et al., 2003) and 5′-CUACAAAGCCCACUACUUU(dTdT)-3′ for $siS1P_2$ (Eurofins MWG Operon, Ebersberg, Germany). Transfection of mCherry–vimentin-encoding plasmids was performed with Lipofectamine LTX (Life Technologies) according to the manufacturer's instructions or with the Gene Pulser Xcell Electroporation System using 25 µg plasmid per transfection. Experiments were performed 48 h post-transfection. Stable cell pools of MDA-MB-435S mCherry–vimentin-transfected cells were made by selection with geneticin. To boost the number of plasmid-expressing cells before experiments, stable cell lines were re-transfected with the appropriate plasmid. mCherry empty vector (EV), vimentin wild-type (WT) and vimentin S71A plasmids were kind gifts from Hong-Chen Chen (Department of Life Sciences and Agricultural Biotechnology Center, National Chung Hsing University, Taichung 402, Taiwan) (Pan et al., 2011).

Chemotactic migration

Boyden chamber migration experiments were conducted with 6.5-mm diameter Transwell Permeable Support inserts and a 8-µm pore size (Corning Inc., Corning, NY). Cells were lipid-starved overnight before the experiments. 100,000 MDA-MB-453S cells, or 50,000 C643 or MEF cells in medium containing 5% lipid-stripped FBS was added to the upper well and 10% lipid-stripped FBS and the vehicle control or sphingolipid to the lower well. MDA-MB-435S cells migrated overnight, C643 and MEF cells for 6 h. Mitomycin C (1 µg/ml, Sigma-Aldrich) was used in MDA-MB-435S migration experiments to prevent proliferation. Non-migrated cells were removed with a cotton swab and the cells were fixed with 2% paraformaldehyde (PFA), stained with Crystal Violet, washed with PBS and Milli-Q water and allowed to dry. Cells were counted at a 40× magnification from eight microscope fields per chamber.

Wound healing imaging with Incucyte ZOOM

Cells were plated in duplicate on 96-well Essen Image Lock plates (Essen BioScience, UK) at 35,000 cells per well and were allowed to adhere for 6 h before lipid-starving overnight. Wounds were made using the Essen WoundMaker (Essen BioScience, UK) and one image was obtained using the Incucyte ZOOM (Essen BioScience, UK) prior to treatment. Cells were treated with S1P, SPC or the appropriate controls and wound closure was monitored by acquiring images every 2 h over a 24 h period with the Incucyte ZOOM. Analysis of wound closure was performed using the Incucyte Scratch Wound Analysis module.

Mass spectrometry

Cells were lysed in SDS buffer, sonicated, boiled and run on a 10% large SDS-PAGE gel with an intermediate filament preparation as a positive control. Gels were stained with Coomassie Blue and destained with methanol and acetic acid. The positive control enabled successful identification and extraction of the vimentin bands stained in the control and treatments.

To identify phosphorylation sites, in-gel digestion with trypsin, TiO_2 affinity chromatography and liquid chromatography-tandem mass spectrometry (LC-MS/MS) were performed as described previously (Imanishi et al., 2007) with some modifications. For LC-MS/MS analysis, an EASY-nLC 1000 nanoflow liquid chromatograph coupled to a Q Exactive mass spectrometer (Thermo Fisher Scientific, Waltham, MA) was used. Database search was performed against the SwissProt (*Homo sapiens*) database and the reversed sequence decoy database using Mascot 2.4 (Matrix Science, London, UK) via Proteome Discoverer 1.3 (Thermo Fisher Scientific). Label-free quantification was performed using Progenesis LC-MS 4.0 (Nonlinear Dynamics, Newcastle upon Tyne, UK).

SDS-PAGE and western blotting

Whole-cell lysates were made with Laemmli sample buffer (LSB). In some experiments, cells were lysed with a lysis buffer (10 mM Tris-HCl, 150 mM NaCl, 7 mM EDTA and 0.5% NP-40) on ice and protein concentrations were measured with the Bradford assay before addition of LSB. Proteins were separated by SDS-PAGE and transferred onto nitrocellulose membrane (Whatman, Maidstone, UK), blocked with 5% fat-free milk in PBS or TBS and incubated overnight with the appropriate antibody. Proteins were detected with enhanced chemiluminescence (Western Lightning Plus-ECL, Perkin Elmer, Waltham, MA). Hsc70 or β-actin was used as a loading control. Levels of phosphorylated proteins were normalised with the non-phosphorylated form and with the loading control. Densitometric analysis of protein bands was done with ImageJ (http://rsbweb.nih.gov/ij/). Antibodies used for western blotting are described in supplementary material Table S2. Positive control lysates for supplementary material Fig. S4 were Caco-2 (kind gift from Dr D. Toivola, Department of Biosciences, Åbo Akademi University, Turku, Finland.), primary myoblasts (Pallari et al., 2011) and HeLa cells [American Type Culture Collection (ATCC), UK].

Immunofluorescence

Cells were grown on glass coverslips and pretreated as indicated. Cells were fixed with 3.7% PFA for 5 min at room temperature, and permeabilised with 0.1% Triton X-100 at room temperature. Blocking was carried out with 10% goat serum (Life Technologies) or 1% BSA (Sigma-Aldrich) for in PBS for 1 h at room temperature. Then coverslips were incubated with primary antibody in blocking solution for 1 h in room temperature or overnight at +4°C. Coverslips were washed three times in PBS and then incubated with an appropriate Alexa-Fluor-conjugated secondary antibody and in some experiments with Alexa-Fluor-conjugated phalloidin in blocking buffer, followed by two washes in PBS, one wash in MilliQ-H_2O and mounting with mowiol. Antibodies used for immunofluorescence are described in supplementary material Table S2.

Cells were imaged with a Leica SP5 laser scanning confocal microscope (Leica, Wetzlar, Germany) using a 60×/1.4 NA plan-apochromat oil immersion objective. The widefield mCherry transfection images were acquired with a Leica DMRE 20× magnification objective.

Cell shape measurements

C643 cells were labelled with CFSE CellTracker dye according to manufacturer instructions prior to sphingolipid treatments. Cells were fixed, mounted and entire cells were imaged with Leica SP5 or Zeiss LSM 780 confocal microscope with a 20× air objective. For cell volume analysis with BioImageXD (Kankaanpää et al., 2012) images were converted into a 512×512 resolution and stacks were segmented to identify individual cells and measure volumes. Objects with less than 500 voxels were removed from the analysis. To measure cell perimeter 3D image stacks were made into maximum projections and the length of the cell perimeter was analysed with CellProfiler (Carpenter et al., 2006).

Fluorescence recovery after photobleaching

FRAP was carried out with Zeiss 780 confocal microscope (Carl Zeiss AG, Jena, Germany) with a 60× water immersion objective. 50,000 MDA-MB-435S cells/well were plated on 35-mm glass-bottomed dishes (MatTek Corporation, Ashland, MA). Cells were transfected with the mCherry–vimentin-WT construct the following day with Lipofectamine LTX (Life Technologies) according to the manufacturer's instructions. The following day, the cells were lipid-starved overnight. FRAP imaging was performed 48 h post-transfection. Bar-shaped 2-µm-wide regions were bleached and recovery was imaged for 15 min at 30-s intervals. The FRAP images were analysed afterwards with ImageJ (measurement of intensity of the bleached spot and control area) followed by FCalc (fitting of the recovery curve and calculation of half-recovery and mobile fraction values). Analysis was performed for areas where individual filaments could be followed from start to finish. The analysis region was moved over time if the cell or the analysed intracellular region moved uniformly. One function fit and correction for bleaching were used for FRAP calculation. The data for the recovery curves was normalised (deduction of background noise and normalization of all experiments to a 0–1 scale). GraphPad Prism was used for fitting of the exponential one-phase association recovery curve.

Quantitative real-time PCR

RNA was isolated with the Aurum Total RNA Mini kit (Bio-Rad Laboratories). NanoDrop 2000 (Thermo Fisher Scientific) was used to measure RNA concentrations and check RNA purity. RNA integrity was confirmed by agarose gel electrophoresis. cDNA was produced from equal amounts of RNA with RevertAid reverse transcriptase (enzyme, dNTPs, random hexamer primers and RiboLock RNase inhibitor were from Thermo Fisher Scientific). The qPCR assay for $S1P_2$ was designed with the Universal Probe Library (UPL) Assay Design Center (www.roche-applied-science.com): 5′-CCACTCGGCAATGTACCTGT-3′ (forward; TAG Copenhagen, Copenhagen, Denmark), 5′-ACGCCTGCCAGTAGATCG-3′ (reverse, TAG Copenhagen) and UPL probe #61 (Roche, Basel, Switzerland). GAPDH was used as a reference gene: 5′-GTTCGACAGTCAGCCGCATC-3′ (forward; Oligomer, Helsinki, Finland), 5′-GGAATTTGCCATGGGTGGA-3′ (reverse, Oligomer), 5′-ACCAGGCGCCCAATACGACCAA-3′ (probe, Oligomer). Quantitative real-time PCR (qPCR) mixtures were prepared with KAPA Probe Fast Master Mix (Kapa Biosystems, Boston, MA) and qPCR was performed with StepOnePlus Real-Time PCR System (Applied Biosystems) using the relative standard curve method.

Wound healing, single-cell motility imaging and analysis with Cell-IQ

C643 and MDA-MB-435S cells were grown on 24-well plates to less than 50% confluency. They were treated as indicated with S1P, SPC, JTE and Y27362 and were imaged using the Cell-IQ (CM Technologies, Finland). Images were collected once an hour over a 20-h period. The videos were analysed by manually tracking cell movements for individual cell speed, directionality and persistence using ImageJ Manual Tracking plugin for 20 cells per video with three independent repeats. Vector plots were created with the Chemotaxis and Migration Tool (Ibidi, Munich, Germany). For the wound healing, wounds were created by plating 20,000 cells in each chamber of wound healing culture inserts (Ibidi) in a 12-well plate. Cells were pretreated with Y27632 as required. On the day of the assay, the insert was removed, cells were treated with sphingolipids and the wound closure was followed every hour. For the single-cell tracking, 20 cells were chosen close to or at the edge of the cells for tracking, with three independent repeats. Cells were manually tracked using the ImageJ Manual Tracking plugin. The data from one side of the wound was inverted to reflect migration from the starting point into the wound. Analysis of directionality, velocity and forward migration index (FMI) was performed using the Chemotaxis and Migration tool (Ibidi).

Statistical analysis

Data are presented as mean±s.e.m. for at least three independent experiments and Student's *t*-test or one- or two-way ANOVA, where appropriate, with either Dunnett's or Bonferroni's *post hoc* test was used for statistical analysis. Analysis was performed and graphs were created with GraphPad Prism 5 (GraphPad, San Diego, CA, USA).

Acknowledgements

Mass spectrometry was performed at the Turku Proteomics Facility. The intermediate filament preparation was made by Ponnuswamy Mohanasundaram from the laboratory of J.E.E.

Competing interests

The authors declare no competing or financial interests.

Author contributions

C.L.H. and K.K. devised the key concepts of the experimental plan under the guidance of J.E.E. and K.T. The Boyden chamber migrations, all western blotting and blot analysis and qPCR experiments were performed by K.K. Live-cell migration imaging, tracking and analysis, confocal imaging and analysis were done by C.L.H. with help from K.K. The mass spectrometry was performed and analysed by S.Y.I. The vimentin phospho-antibodies were generated by H.G. and M.I., who also provided manuscript advice. K.I. performed the cell perimeter and FRAP experiments and analysis. E.F. assisted with confocal imaging and analysis. C.L.H., K.K., S.Y.I., K.I., E.F. generated the figures. C.L.H. and K.K. co-wrote the article with J.E.E. and K.T. The J.E.E. and K.T. laboratories had equal contribution.

Funding

This study was supported by the Sigrid Jusélius Foundation; the Liv och Hälsa Foundation; The Academy of Finland; the Centre of Excellence in Cell Stress and Molecular Ageing (Åbo Akademi University); Åbo Akademi University; Finnish Cultural Foundation; Ida Montin Foundation; the K. Albin Johansson Foundation; the Tor, Joe and Pentti Borg Foundation; the Arvid and Greta Olin Foundation; and the Receptor Research Program (Åbo Akademi University and the University of Turku).

Supplementary material

Supplementary material available online at
http://jcs.biologists.org/lookup/suppl/doi:10.1242/jcs.160341/-/DC1

References

Adada, M., Canals, D., Hannun, Y. A. and Obeid, L. M. (2013). Sphingosine-1-phosphate receptor 2. *FEBS J.* **280**, 6354-6366.

Alewijnse, A. E. and Michel, M. C. (2006). Sphingosine-1-phosphate and sphingosylphosphorylcholine: two of a kind? *Br. J. Pharmacol.* **147**, 347-348.

Alix-Panabières, C., Vendrell, J.-P., Slijper, M., Pellé, O., Barbotte, E., Mercier, G., Jacot, W., Fabbro, M. and Pantel, K. (2009). Full-length cytokeratin-19 is released by human tumor cells: a potential role in metastatic progression of breast cancer. *Breast Cancer Res.* **11**, R39.

Alvarez, S. E., Harikumar, K. B., Hait, N. C., Allegood, J., Strub, G. M., Kim, E. Y., Maceyka, M., Jiang, H., Luo, C., Kordula, T. et al. (2010). Sphingosine-1-phosphate is a missing cofactor for the E3 ubiquitin ligase TRAF2. *Nature* **465**, 1084-1088.

Amano, M., Nakayama, M. and Kaibuchi, K. (2010). Rho-kinase/ROCK: A key regulator of the cytoskeleton and cell polarity. *Cytoskeleton* **67**, 545-554.

Asghar, M. Y., Viitanen, T., Kemppainen, K. and Törnquist, K. (2012). Sphingosine 1-phosphate and human ether-a'-go-go-related gene potassium channels modulate migration in human anaplastic thyroid cancer cells. *Endocr. Relat. Cancer* **19**, 667-680.

Barberis, L., Pasquali, C., Bertschy-Meier, D., Cuccurullo, A., Costa, C., Ambrogio, C., Vilbois, F., Chiarle, R., Wymann, M., Altruda, F. et al. (2009). Leukocyte transmigration is modulated by chemokine-mediated PI3Kgamma-dependent phosphorylation of vimentin. *Eur. J. Immunol.* **39**, 1136-1146.

Bauer, P. O., Hudec, R., Goswami, A., Kurosawa, M., Matsumoto, G., Mikoshiba, K. and Nukina, N. (2012). ROCK-phosphorylated vimentin modifies mutant huntingtin aggregation via sequestration of IRBIT. *Mol. Neurodegener.* **7**, 43.

Beil, M., Micoulet, A., von Wichert, G., Paschke, S., Walther, P., Omary, M. B., Van Veldhoven, P. P., Gern, U., Wolff-Hieber, E., Eggermann, J. et al. (2003). Sphingosylphosphorylcholine regulates keratin network architecture and visco-elastic properties of human cancer cells. *Nat. Cell Biol.* **5**, 803-811.

Berra, E., Benizri, E., Ginouvès, A., Volmat, V., Roux, D. and Pouysségur, J. (2003). HIF prolyl-hydroxylase 2 is the key oxygen sensor setting low steady-state levels of HIF-1alpha in normoxia. *EMBO J.* **22**, 4082-4090.

Busch, T., Armacki, M., Eiseler, T., Joodi, G., Temme, C., Jansen, J., von Wichert, G., Omary, M. B., Spatz, J. and Seufferlein, T. (2012). Keratin 8 phosphorylation regulates keratin reorganization and migration of epithelial tumor cells. *J. Cell Sci.* **125**, 2148-2159.

Carpenter, A. E., Jones, T.R., Lamprecht, M. R., Clarke, C., Kang, I. H., Friman, O., Guertin, D. A., Chang, J. H., Lindquist, R. A., Moffat, J., Golland, P. and Sabatini, D. M. (2006). CellProfiler: image analysis software for identifying and quantifying cell phenotypes. *Genome Biol.* **7**:R100.

Chernoivanenko, I. S., Minin, A. A. and Minin, A. A. (2013). [Role of vimentin in cell migration]. *Ontogenez* **44**, 186-202.

Chung, B.-M., Rotty, J. D. and Coulombe, P. A. (2013). Networking galore: intermediate filaments and cell migration. *Curr. Opin. Cell Biol.* **25**, 600-612.

Dave, J. M., Kang, H., Abbey, C. A., Maxwell, S. A. and Bayless, K. J. (2013). Proteomic profiling of endothelial invasion revealed receptor for activated C kinase 1 (RACK1) complexed with vimentin to regulate focal adhesion kinase (FAK). *J. Biol. Chem.* **288**, 30720-30733.

Eckes, B., Dogic, D., Colucci-Guyon, E., Wang, N., Maniotis, A., Ingber, D., Merckling, A., Langa, F., Aumailley, M., Delouvée, A., et al. (1998). Impaired mechanical stability, migration and contractile capacity in vimentin-deficient fibroblasts. *J. Cell Sci.* **111**, 1897-1907.

Eckes, B., Colucci-Guyon, E., Smola, H., Nodder, S., Babinet, C., Krieg, T. and Martin, P. (2000). Impaired wound healing in embryonic and adult mice lacking vimentin. *J. Cell Sci.* **113**, 2455-2462.

Eriksson, J. E., He, T., Trejo-Skalli, A. V., Härmälä-Braskén, A.-S., Hellman, J., Chou, Y.-H. and Goldman, R. D. (2004). Specific in vivo phosphorylation sites determine the assembly dynamics of vimentin intermediate filaments. *J. Cell Sci.* **117**, 919-932.

Fois, G., Weimer, M., Busch, T., Felder, E. T., Oswald, F., von Wichert, G., Seufferlein, T., Dietl, P. and Felder, E. (2013). Effects of keratin phosphorylation on the mechanical properties of keratin filaments in living cells. *FASEB J.* **27**, 1322-1329.

Goto, H., Kosako, H., Tanabe, K., Yanagida, M., Sakurai, M., Amano, M., Kaibuchi, K. and Inagaki, M. (1998). Phosphorylation of vimentin by Rho-associated kinase at a unique amino-terminal site that is specifically phosphorylated during cytokinesis. *J. Biol. Chem.* **273**, 11728-11736.

Hait, N. C., Allegood, J., Maceyka, M., Strub, G. M., Harikumar, K. B., Singh, S. K., Luo, C., Marmorstein, R., Kordula, T., Milstien, S. et al. (2009). Regulation of histone acetylation in the nucleus by sphingosine-1-phosphate. *Science* **325**, 1254-1257.

Helfand, B. T., Mendez, M. G., Murthy, S. N. P., Shumaker, D. K., Grin, B., Mahammad, S., Aebi, U., Wedig, T., Wu, Y. I., Hahn, K. M. et al. (2011). Vimentin organization modulates the formation of lamellipodia. *Mol. Biol. Cell* **22**, 1274-1289.

Hyder, C. L., Pallari, H.-M., Kochin, V. and Eriksson, J. E. (2008). Providing cellular signposts—post-translational modifications of intermediate filaments. *FEBS Lett.* **582**, 2140-2148.

Hyder, C. L., Isoniemi, K. O., Torvaldson, E. S. and Eriksson, J. E. (2011). Insights into intermediate filament regulation from development to ageing. *J. Cell Sci.* **124**, 1363-1372.

Imanishi, S. Y., Kochin, V., Ferraris, S. E., de Thonel, A., Pallari, H.-M., Corthals, G. L. and Eriksson, J. E. (2007). Reference-facilitated phosphoproteomics: fast and reliable phosphopeptide validation by microLC-ESI-Q-TOF MS/MS. *Mol. Cell. Proteomics* **6**, 1380-1391.

Inada, H., Togashi, H., Nakamura, Y., Kaibuchi, K., Nagata, K. and Inagaki, M. (1999). Balance between activities of Rho kinase and type 1 protein phosphatase modulates turnover of phosphorylation and dynamics of desmin/vimentin filaments. *J. Biol. Chem.* **274**, 34932-34939.

Ivaska, J. (2011). Vimentin: central hub in EMT induction? *Small GTPases* 2, 51–53.

Ivaska, J., Vuoriluoto, K., Huovinen, T., Izawa, I., Inagaki, M. and Parker, P. J. (2005). PKCepsilon-mediated phosphorylation of vimentin controls integrin recycling and motility. *EMBO J.* **24**, 3834-3845.

Ivaska, J., Pallari, H.-M., Nevo, J. and Eriksson, J. E. (2007). Novel functions of vimentin in cell adhesion, migration, and signaling. *Exp. Cell Res.* **313**, 2050-2062.

Iyer, S. V., Dange, P. P., Alam, H., Sawant, S. S., Ingle, A. D., Borges, A. M., Shirsat, N. V., Dalal, S. N. and Vaidya, M. M. (2013). Understanding the role of keratins 8 and 18 in neoplastic potential of breast cancer derived cell lines. *PLoS ONE* **8**, e53532.

Izawa, I. and Inagaki, M. (2006). Regulatory mechanisms and functions of intermediate filaments: a study using site- and phosphorylation state-specific antibodies. *Cancer Sci.* **97**, 167-174.

Kankaanpää, P., Paavolainen, L., Tiitta, S., Karjalainen, M., Päivärinne, J., Nieminen, J., Marjomäki, V., Heino, J. and White, D. J. (2012). BioImageXD: an open, general-purpose and high-throughput image-processing platform. *Nat. Methods* **9**, 683-689.

Kim, H., Nakamura, F., Lee, W., Shifrin, Y., Arora, P. and McCulloch, C. A. (2010). Filamin A is required for vimentin-mediated cell adhesion and spreading. *Am. J. Physiol.* **298**, C221-C236.

Lei, S., Tian, Y.-P., Xiao, W.-D., Li, S., Rao, X.-C., Zhang, J.-L., Yang, J., Hu, X.-M. and Chen, W. (2013). ROCK is involved in vimentin phosphorylation and rearrangement induced by dengue virus. *Cell Biochem. Biophys.* **67**, 1333-1342.

Lepley, D., Paik, J.-H., Hla, T. and Ferrer, F. (2005). The G protein-coupled receptor S1P2 regulates Rho/Rho kinase pathway to inhibit tumor cell migration. *Cancer Res.* **65**, 3788-3795.

Li, J., Guo, B., Wang, J., Cheng, X., Xu, Y. and Sang, J. (2013). Ovarian cancer G protein coupled receptor 1 suppresses cell migration of MCF7 breast cancer cells via a Gα12/13-Rho-Rac1 pathway. *J. Mol. Signal.* **8**, 6.

Loirand, G., Guérin, P. and Pacaud, P. (2006). Rho kinases in cardiovascular physiology and pathophysiology. *Circ. Res.* **98**, 322-334.

Lund, N., Henrion, D., Tiede, P., Ziche, M., Schunkert, H. and Ito, W. D. (2010). Vimentin expression influences flow dependent VASP phosphorylation and regulates cell migration and proliferation. *Biochem. Biophys. Res. Commun.* **395**, 401-406.

Mendez, M. G., Kojima, S. and Goldman, R. D. (2010). Vimentin induces changes in cell shape, motility, and adhesion during the epithelial to mesenchymal transition. *FASEB J.* **24**, 1838-1851.

Meyer zu Heringdorf, D. and Jakobs, K. H. (2007). Lysophospholipid receptors: signalling, pharmacology and regulation by lysophospholipid metabolism. *Biochim. Biophys. Acta* **1768**, 923-940.

Nakamura, Y., Hashimoto, R., Amano, M., Nagata, K., Matsumoto, N., Goto, H., Fukusho, E., Mori, H., Kashiwagi, Y., Kudo, T. et al. (2000). Localized phosphorylation of vimentin by rho-kinase in neuroblastoma N2a cells. *Genes Cells* **5**, 823-837.

Nieminen, M., Henttinen, T., Merinen, M., Marttila-Ichihara, F., Eriksson, J. E. and Jalkanen, S. (2006). Vimentin function in lymphocyte adhesion and transcellular migration. *Nat. Cell Biol.* **8**, 156-162.

Nixon, G. F., Mathieson, F. A. and Hunter, I. (2008). The multi-functional role of sphingosylphosphorylcholine. *Prog. Lipid Res.* **47**, 62-75.

Pallari, H.-M. and Eriksson, J. E. (2006). Intermediate filaments as signaling platforms. *Sci. STKE* **2006**, e53.

Pallari, H.-M., Lindqvist, J., Torvaldson, E., Ferraris, S. E., He, T., Sahlgren, C. and Eriksson, J. E. (2011). Nestin as a regulator of Cdk5 in differentiating myoblasts. *Mol. Biol. Cell*, **22**, 1539-1549.

Pan, Y.-R., Chen, C.-L. and Chen, H.-C. (2011). FAK is required for the assembly of podosome rosettes. *J. Cell Biol.* **195**, 113-129.

Park, M. K., Lee, H. J., Shin, J., Noh, M., Kim, S. Y. and Lee, C. H. (2011). Novel participation of transglutaminase-2 through c-Jun N-terminal kinase activation in sphingosylphosphorylcholine-induced keratin reorganization of PANC-1 cells. *Biochim. Biophys. Acta* **1811**, 1021-1029.

Pyne, N. J. and Pyne, S. (2010). Sphingosine 1-phosphate and cancer. *Nat. Rev. Cancer* **10**, 489-503.

Robert, A., Herrmann, H., Davidson, M. W. and Gelfand, V. I. (2014). Microtubule-dependent transport of vimentin filament precursors is regulated by actin and by the concerted action of Rho- and p21-activated kinases. *FASEB J.* **28**, 2879-2890.

Satelli, A. and Li, S. (2011). Vimentin in cancer and its potential as a molecular target for cancer therapy. *Cell. Mol. Life Sci.* **68**, 3033-3046.

Sellappan, S., Grijalva, R., Zhou, X., Yang, W., Eli, M. B., Mills, G. B. and Yu, D. (2004). Lineage infidelity of MDA-MB-435 cells: expression of melanocyte proteins in a breast cancer cell line. *Cancer Res.* **64**, 3479-3485.

Shi, J. and Wei, L. (2007). Rho kinase in the regulation of cell death and survival. *Arch. Immunol. Ther. Exp. (Warsz).* **55**, 61-75.

Sin, W. C., Chen, X. Q., Leung, T. and Lim, L. (1998). RhoA-binding kinase alpha translocation is facilitated by the collapse of the vimentin intermediate filament network. *Mol. Cell. Biol.* **18**, 6325-6339.

Snider, N. T. and Omary, M. B. (2014). Post-translational modifications of intermediate filament proteins: mechanisms and functions. *Nat. Rev. Mol. Cell Biol.* **15**, 163-177.

Svitkina, T. M., Verkhovsky, A. B. and Borisy, G. G. (1996). Plectin sidearms mediate interaction of intermediate filaments with microtubules and other components of the cytoskeleton. *J. Cell Biol.* **135**, 991-1007.

Tobo, M., Tomura, H., Mogi, C., Wang, J.-Q., Liu, J.-P., Komachi, M., Damirin, A., Kimura, T., Murata, N., Kurose, H. et al. (2007). Previously postulated "ligand-independent" signaling of GPR4 is mediated through proton-sensing mechanisms. *Cell. Signal.* **19**, 1745-1753.

Yokoyama, T., Goto, H., Izawa, I., Mizutani, H. and Inagaki, M. (2005). Aurora-B and Rho-kinase/ROCK, the two cleavage furrow kinases, independently regulate the progression of cytokinesis: possible existence of a novel cleavage furrow kinase phosphorylates ezrin/radixin/moesin (ERM). *Genes Cells* **10**, 127-137.

Yoon, M., Moir, R. D., Prahlad, V. and Goldman, R. D. (1998). Motile properties of vimentin intermediate filament networks in living cells. *J. Cell Biol.* **143**, 147-157.